Tetrahedron 66 (2010) 3199–3206

Contents lists available at ScienceDirect

Tetrahedron

journal homepage: www.elsevier.com/locate/tet

Easily functionalizable carbazole based building blocks with extended conjugated systems for optoelectronic applications

Giedre Bubniene [a], Tadas Malinauskas [a], Maryte Daskeviciene [a], Vygintas Jankauskas [b], Vytautas Getautis [a,*]

[a] Department of Organic Chemistry, Kaunas University of Technology, Radvilenu pl. 19, LT-50270 Kaunas, Lithuania
[b] Department of Solid State Electronics, Vilnius University, Sauletekio 9, LT-10222, Vilnius, Lithuania

ARTICLE INFO

Article history:
Received 10 December 2009
Received in revised form 2 February 2010
Accepted 22 February 2010
Available online 25 February 2010

Keywords:
Carbazole
Diphenylacetaldehyde
Charge transport
Ionization energy

ABSTRACT

Carbazole based building blocks, possessing diphenylethenyl fragments, have been synthesized. Condensation of the carbazol-2-ol with diphenylacetaldehyde yields 1,3-substituted derivatives. Change of the synthesis sequence, however, (i.e., substitution at the hydroxyl and NH groups, followed by the condensation reaction) results in the 3,6-substituted products. Thermal, optical, electrochemical and photophysical properties of the synthesized derivatives have been investigated. Room temperature hole-drift mobilities, evaluated using xerographic time-of-flight technique, were found to exceed 10^{-4} $cm^2 V^{-1} s^{-1}$ at strong electric fields. The obtained results indicate high charge mobility for molecularly doped polymers, especially considering the fact that these measurements were carried out under ambient conditions and not in high vacuum. Commercial availability and relative cheapness of the starting materials, simple synthetic method, number of sites available for easy functionalization and covalent linking to other molecules makes these precursors attractive building blocks for the construction of more complex low-molecular-weight or polymeric materials for optoelectronic applications.

1. Introduction

Electronic and optoelectronic devices using organic materials as active elements, for example, organic light-emitting diodes (OLEDs), organic photovoltaic devices (OPVs), organic field-effect transistors (OFETs), organic photorefractive devices, and so forth, have recently received a great deal of attention from the standpoint of potential technological applications as well as fundamental science.[1] The devices using organic materials are attractive because they can take advantage of organic materials such as light weight, potentially low cost, thin-film capable, large-area, flexible device fabrication.

Due to their specific optical and electrochemical properties, carbazole and its derivatives have been widely used as functional building blocks in the fabrication of various optoelectronic devices.[2] In the field of OLED technology, carbazole derivatives are usually used as promising blue light-emitting materials.[3]

Interestingly, white light is also achieved from carbazole dimers or oligomers serving as a single-emitting-component layer.[4]

Meanwhile, a great many carbazole homopolymers or oligomers, as well as carbazole-containing polymers or small molecules, are of excellent hole transport ability, due to their electron-donating capabilities.[5] Furthermore, carbazole derivatives are of high triplet energy and capable of functioning as host materials in highly efficient blue, green, or red electrophosphorescent devices,[6] due to the efficient energy transfer from these hosts to doped triplet emitters.

The carbazole moiety can be easily functionalized or covalently linked to other molecules. Numerous ways are known for enhancement of its conjugated π-electron system. For instance, 3,6- or 2,7-linking of carbazole molecules into dimers, trimers or oligomers,[7a,b] and addition of enamine,[7c] hydrazone[7d–f] or diarylamino[2a] fragments.

An efficient carbazole based building block for the synthesis of more complex, low-molecular-weight or polymeric materials designed for optoelectronic applications, should be easily functionalizable and possess good charge transport properties. Apart from the factors mentioned above, other important requirements are: relatively low cost and commercial availability of starting materials as well as simple and easy synthesis on a multigram scale.

Preliminary research results on this type of building blocks have been reported by us recently.[8] Herein, we present the detailed synthesis and photophysical properties of the new carbazole based precursors with increased π-conjugated systems, who meet all of the mentioned conditions.

* Corresponding author. Tel.: +370 37 300196; fax: +370 37 300152.
E-mail address: vgetaut@ktu.lt (V. Getautis).

0040-4020/$ – see front matter © 2010 Elsevier Ltd. All rights reserved.
doi:10.1016/j.tet.2010.02.086

2. Results and discussion

2.1. Synthesis

Condensation of 9*H*-carbazol-2-ol with diphenylacetaldehyde in 1,4-dioxane (water generated during the course of the reaction was removed with 4 Å molecular sieves) at a reflux temperature results in formation of 1,3-bis(2,2-diphenylethenyl)-9*H*-carbazol-2-ol (**1**) (Scheme 1). The presence of the strongly *ortho*/*para*-directing hydroxyl group activates the 1- and 3-positions of the carbazole ring, and the reaction is more likely to proceed at those sites.

Most probably, delocalization of the lone pair pushes electrons from the nitrogen atom into the ring and the heterocycle becomes electron-rich at the expense of the nitrogen atom. An obvious consequence of this delocalization is the increased acidity of the NH group as a whole; therefore, protonation does not occur at the nitrogen atom when using an acid catalyst. The nucleophilic nature of the ring means that carbazole is attacked readily by electrophiles, this is further enhanced by the presence of the electron-donating hydroxyl group at the 2-position. Because nitrogen is less electronegative than oxygen, the lone pair is higher in energy and so more available to interact with the π system than the lone pair on oxygen. Delocalization increases the δ^- charge on the carbon atoms at the 1- and 3-positions of the 2-hydroxycarbazole molecule, and these positions are more susceptible to the electrophilic attack (Scheme 2).

During the electrophilic substitution, a σ bond is formed between diphenylacetaldehyde and 2-hydroxycarbazole, the carbonyl π bond polarized leaving an oxyanion (alkoxide) and an iminium cation is created. This is followed by a loss of a proton at the 1-position of the carbazole ring, and acceptance of a proton by the formed alkoxide ion to form the hydroxyl group. Protonation of the

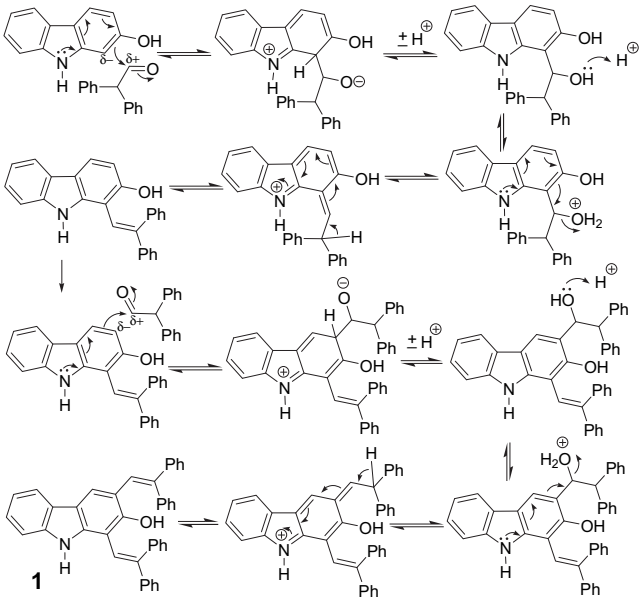

Scheme 2. Proposed reaction mechanism.

hydroxyl group and subsequent loss of water by elimination followed by the loss of a proton leads to the formation of the monosubstituted compound. Identically, reaction at the 3-position follows the same route. Theoretical calculations indicate that the δ^- charge is slightly larger at the 1-position, therefore reaction is somewhat more likely to proceed at this position first. However, synthetic experiments showed that disubstituted derivative **1** is

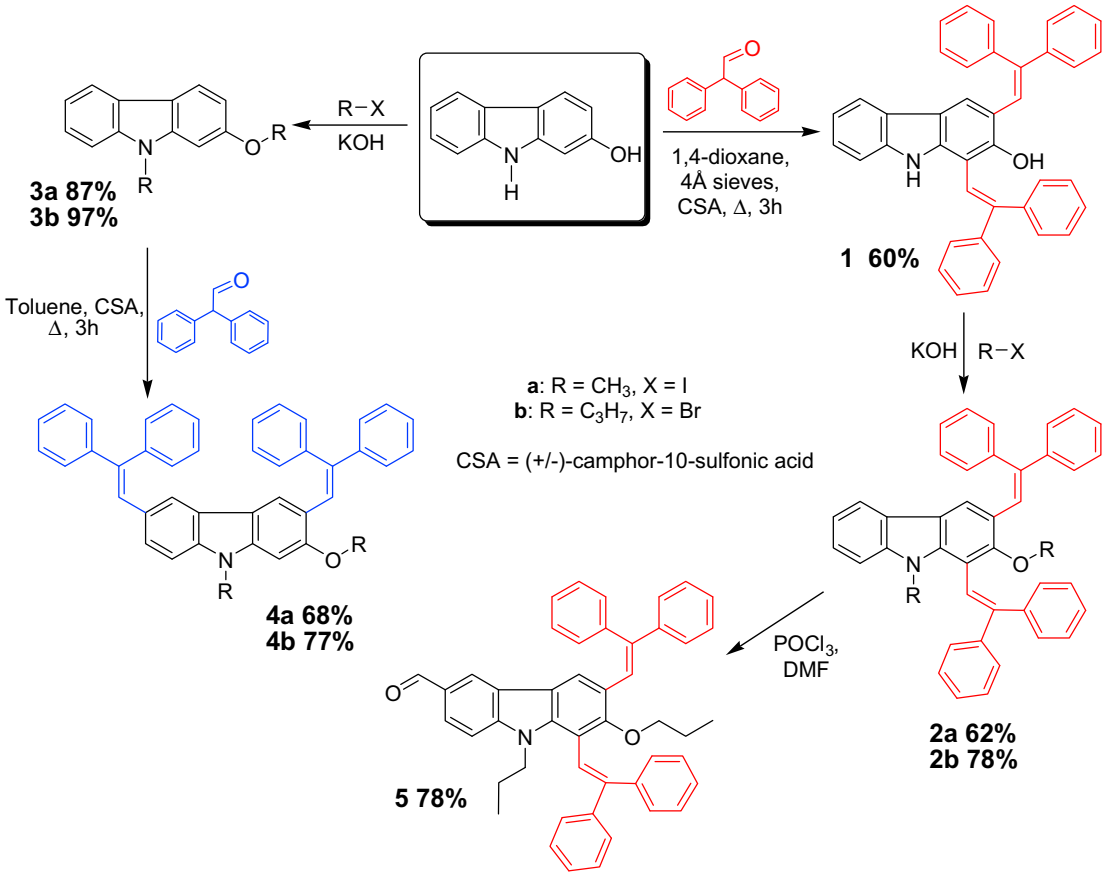

Scheme 1. Synthesis of 1,3- and 3,6-substituted carbazole based precursors **2a**,**b** and **4a**,**b**.

readily formed even when an excess of 9*H*-carbazol-2-ol is used; consequently, reactivity at both positions is quite similar.

The isolated 1,3-disubstituted derivative **1** possesses reactive hydroxyl and NH groups, as well as an unsubstituted 6-position of the carbazole, which is activated by the nitrogen atom. In order to investigate the photophysical properties of the synthesized precursor and test the reactivity of hydroxyl group, as it is located between two bulky substituents, simple alkylation reactions were performed. Reaction of **1** with iodomethane and 1-bromopropane, in the presence of KOH, yielded alkylated carbazole derivatives **2a**,**b**.

Additionally, Vilsmeier formylation of **2b** was also performed to confirm that the 6-position of the carbazole remained active for electrophilic substitution reactions. 1,3,6-Trisubstituted 2-hydroxycarbazole derivative **5** was successfully obtained.

Changing the synthetic sequence, however, (i.e., substitution at hydroxyl and NH groups, followed by the condensation reaction) results in products of a different structure. In this case, condensation of the alkylated intermediate derivatives **3a**,**b** with diphenylacetaldehyde yields 3,6-disubstituted carbazoles **4a**,**b**.

Apparently, substitution of the strongly *ortho*/*para*-directing hydroxyl group with a moderate alkoxyl one, and the additional steric hindrance resulting from such a change, prevent the reaction from proceeding at the 1-position of the carbazole ring. Structural evidence for compounds **2a**,**b** and **4a**,**b** were obtained by NMR spectroscopy. Furthermore, suitable single crystals of **2b** and **4b** were grown from mixtures of *n*-hexane/acetone and THF/2-propanol accordingly, and both structures were proven unambiguously by X-ray crystallography (Fig. 1).

2.2. Thermal analysis

Both 1,3- and 3,6-substituted derivatives of 2-hydroxycarbazole are soluble in common organic solvents such as THF, toluene and chloroform. The thermal properties of the alkylated precursors were determined by differential scanning calorimetry (DSC) and thermogravimetric analysis (TGA) measurements (Table 1). TGA shows that all compounds exhibit high thermal stability. In a nitrogen atmosphere, decomposition starts above 360 °C and 410 °C for **2a**,**b** and **4a**,**b**, respectively. DSC measurements (Supplementary data Fig. S1, S2) indicate that both 1,3- and 3,6-substituted carbazole derivatives are able to form molecular glasses.

In general, glass transition temperatures were higher for the 3,6-substituted derivatives **4a**,**b**, compared with the 1,3-substituted **2a**,**b**. Most likely this is a consequence of tighter packing of the molecules in the compounds **4a**,**b**. Obviously, introduction of longer flexible aliphatic chains leads to the decrease of T_g in both cases.

2.3. The optical, electrochemical and photophysical properties

The UV–vis absorption spectra of the carbazole derivatives **2a**,**b** and **4a**,**b** were recorded at room temperature in THF (Table 1, Fig. 2). The absorption spectra of both **2b** and **4b** are bathochromically shifted ($\approx$22 nm) with respect to the spectrum of 9-ethylcarbazole (λ_{max}=294 nm). Specifically, the $\pi \rightarrow \pi^*$ absorption band is intensified (hyperchromic shift) and shifted to lower energy, indicating extended conjugation in these compounds.

The fluorescence spectra of the carbazole based precursors **2b** and **4b** are also included in Figure 2. The shape and the maxima of the fluorescence curves are almost identical, fluorescence maxima are detected at 476 and 474 nm, respectively. The carbazole derivatives exhibit blue fluorescence, which is usual for carbazole-containing compounds.

The ionization energy (E_I) was measured by the electron photoemission in air method,[9] and results are presented in Table 2. Usually the photoemission experiments are carried out in vacuum, and high vacuum is one of the main requirements for these measurements. If the vacuum is not high enough, the sample surface oxidation and gas adsorption are influencing the measurement results. In our case, however, the organic materials investigated are stable enough to oxygen and the measurements may be carried out in air. The measured ionization energies vary in the range from 5.62 eV to 5.50 eV.

To elucidate the energetic conditions for energy and electron transfer in dilute solutions, the HOMO/LUMO values were also determined using cyclic voltammetry (CV). These E_{HOMO} values do not represent any absolute solid-state or gas-phase ionization energies, but can be used to compare different compounds relative to one another. The cyclic voltammograms of the synthesized compounds in dichloromethane show one quasi-reversible oxidation couple and no reduction waves (Fig. 3). The electrochemical data are summarized in Table 2.

The 1,3-substituted derivative **2b** shows an oxidation peak corresponding to 0.59 V vs Fc, which results in a E_{HOMO} value of −5.32 eV (on the basis of the E_{HOMO} energy level of ferrocene as 4.8 eV). Similarly, compound **4b** exhibits an oxidation at 0.52 V vs Fc. This gives a E_{HOMO} value of −5.23 eV for the compound **4b**. Results from both CV and photoemission in air methods indicate that E_{HOMO} energy level of 3,6-substituted carbazole derivatives **4a**,**b** is slightly lower than that of 1,3-substituted ones (**2a**,**b**).

Charge transport properties of the molecularly doped polymers consisting of 1,3-substituted (**2a**,**b**) or 3,6-substituted (**4a**,**b**) carbazole derivatives, and bisphenol Z polycarbonate (PC-Z) as polymer host (50% solid solutions) were studied by the xerographic time-of-flight (XTOF) technique.[10]

For the solid solution in PC-Z, electron mobility μ may be calculated using the formula:

$$\mu = \mu_0 \exp\left(\alpha\sqrt{E}\right) \quad (1)$$

where μ_0 is the zero field mobility, α is the Poole–Frenkel parameter and E is the electric field strength. The values of charge mobility defining parameters μ_0, α and the mobility at the electric field of 10^6 V cm^{-1} for the compounds **2a**,**b** and **4a**,**b** are given in Table 3.

The examples of the dU/dt transients for the corresponding PC-Z blends are shown in Figure 4. XTOF measurements reveal that small charge transport transients are with a well-defined transit time on linear plots in case of **4b**. The XTOF transients for the compounds **2a**,**b** and **4a**, on the other hand, were of disperse character, but the transit time was well seen on lg–lg plots.

Room temperature hole-drift mobilities were found to approach 10^{-4} cm^2 V^{-1} s^{-1} at strong electric fields (Fig. 5). Presence of longer flexible aliphatic chains in compounds **2b** and **4b** ensures better quality of the obtained layers and consequently noticeably higher hole-drift mobility.

In general, the obtained results indicate high charge mobility for molecularly doped polymers, especially considering the fact that these measurements were carried out under ambient conditions and not in high vacuum.

3. Conclusion

In conclusion, novel carbazole based derivatives possessing diphenylethenyl fragments have been synthesized. Commercial availability and relative cheapness of the starting materials, simple synthetic method, number of sites available for easy functionalization and covalent linking to other molecules, glass-forming properties, good charge drift mobility and solubility in common organic solvents makes these precursors attractive building blocks for the construction of more complex low-molecular-weight or polymeric materials for optoelectronic applications.

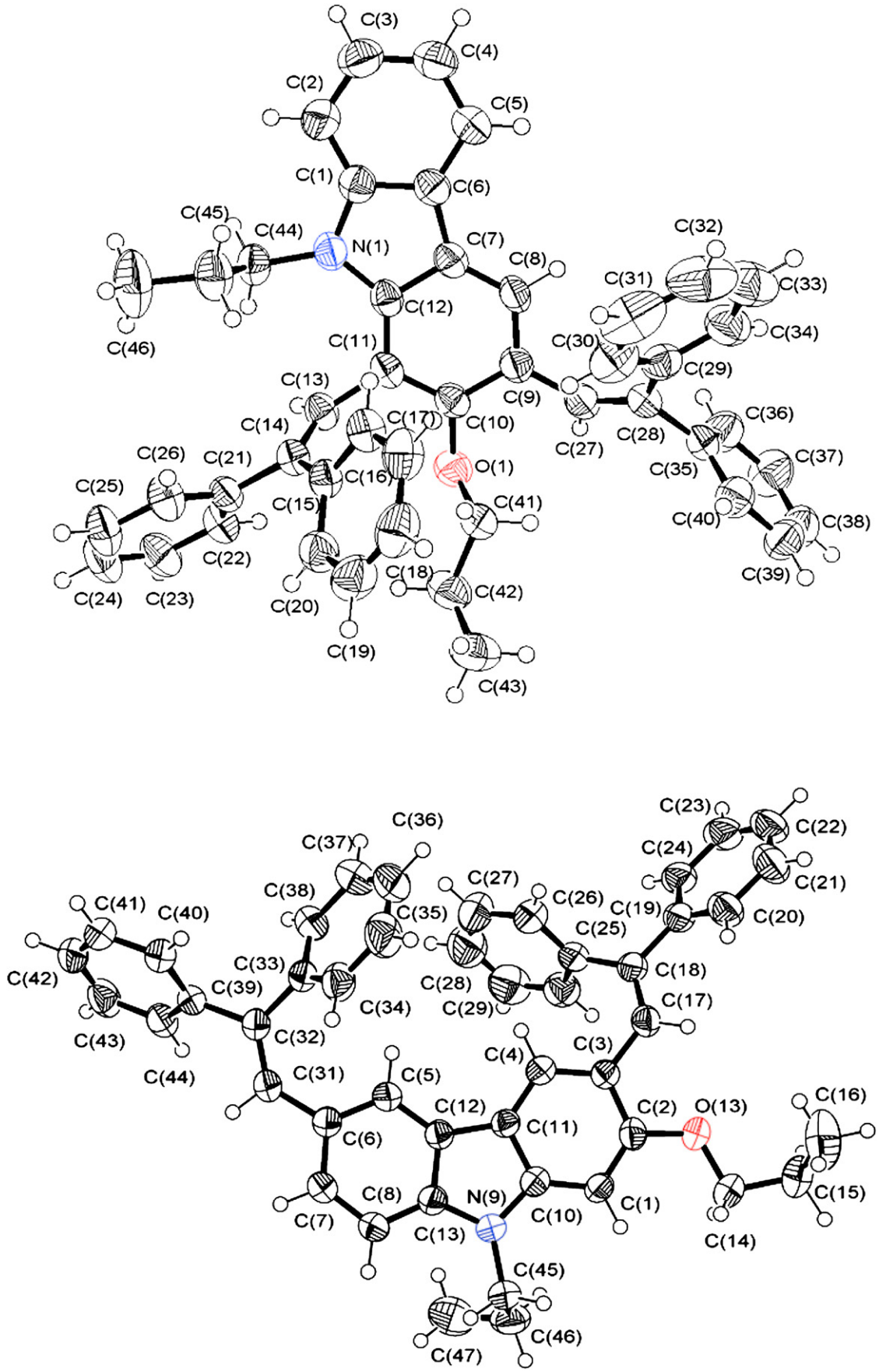

Figure 1. ORTEP projection of the crystal structure of **2b** (top) and **4b** (bottom). Displacement ellipsoids are drawn at 50% probability level.

Table 1
Optical and thermal characteristics of the synthesized derivatives

Entry	λ^{ab}_{max}/nm[a]	ϵ/M^{-1}cm^{-1}	λ^{fl}_{max}/nm[b]	T_g/°C[c]	T_{dec}/°C[d]	T_m/°C[e]
2a	316	2.1×10^4	476	87	365	212
2b	316	2.8×10^4	476	64	369	144
4a	316	2.4×10^4	474	96	415	230
4b	316	3.7×10^4	474	72	413	195

[a] UV–vis and FL spectra measured in 10^{-4} M THF solution.
[b] λ_{ex}=330 nm.
[c] Determined by DSC: scan rate, 10 K/min; N_2 atmosphere; second run.
[d] Onset of decomposition determined by TGA: heating rate, 10 K/min; N_2 atmosphere.
[e] Melting point was only detected during the first heating; the compound vitrified on cooling to room temperature with 10 K/min.

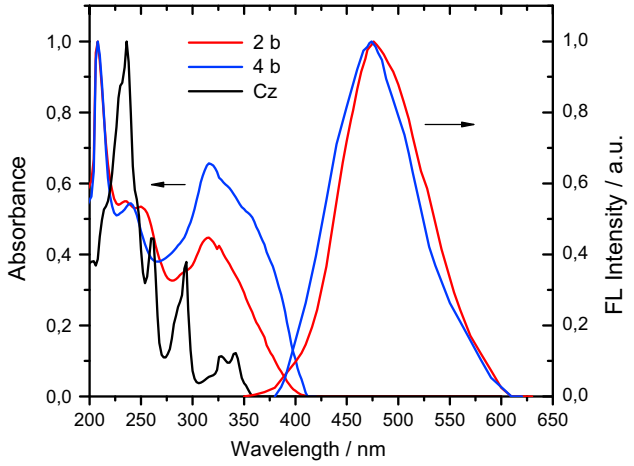

Figure 2. Absorption and fluorescence spectra of 10^{-4} M THF solutions of the carbazole derivatives **2b** and **4b**. The absorption spectrum of 9-ethylcarbazole (Cz) is shown for comparison.

Table 2
HOMO, LUMO, band gap energies and electrochemical properties of **2a**,**b** and **4a**,**b**[a]

Entry	$E_{1/2}$ vs Fc/V[b]	E_{onset} vs Fc/V	E^{ox}_{pc} vs Fc/V	E^{ox}_{pa} vs Fc/V	E^{opt}_g/eV[c]	E_I/eV[d]	E_{HOMO}/eV[e]	E_{LUMO}/eV[f]
2a	0.53	0.46	0.60	0.46	2.99	5.62	−5.33	−2.34
2b	0.52	0.45	0.59	0.45	3.01	5.60	−5.32	−2.31
4a	0.45	0.38	0.55	0.35	2.96	5.56	−5.25	−2.29
4b	0.43	0.36	0.52	0.34	2.97	5.50	−5.23	−2.26

[a] The measurements were carried out at a glassy carbon electrode in dichloromethane solutions containing 0.1 M tetrabutylammonium perchlorate as electrolyte and $Ag/AgNO_3$ as the reference electrode. Each measurement was calibrated with ferrocene (Fc), with the measured $E^{Fc}_{1/2}$=0.105 V vs $Ag/AgNO_3$.
[b] $E_{1/2}=(E_{pa}+E_{pc})/2$; E_{pa} and E_{pc} are peak anodic and peak cathodic potentials, respectively.
[c] The optical band gaps E^{opt}_g estimated from the edges of electronic absorption spectra.
[d] Ionization energy was measured by the photoemission in air method from films.
[e] $E_{HOMO}=4.8+(E_{1/2}-E^{Fc}_{1/2})$.
[f] $E_{LUMO}=E_{HOMO}-E^{opt}_g$.

4. Experimental section

4.1. General

All chemicals were purchased from Aldrich and used as received without further purification. The ^{1}H NMR spectra were recorded on a Varian Unity Inova (300 MHz) spectrometer at room temperature. All the data are given as chemical shifts in δ (ppm), $(CH_3)_4Si$ (TMS, 0 ppm) was used as an internal standard. The course of the reactions products were monitored by TLC on ALUGRAM SIL G/UV254 plates and developed with I_2 or UV light. Silica gel (grade 62, 60–200 mesh, 150 Å, Aldrich) was used for column chromatography. Elemental analysis was performed with an Exeter Analytical CE-440 Elemental. IR-spectroscopy was performed on a Perkin Elmer Spectrum BX II FTIR System, using KBr pellets. X-ray crystallography analysis was carried out utilizing Bruker-Nonius Kappa CCD single crystal diffractometer, using Mo K_α radiation (λ=0.71073 Å). Single crystal data was processed using maXus, SIR 97, ORTEP, SHELXL-97 software. Melting points were determined using Electrothermal MelTemp melting point apparatus. MS were recorded on an Aligent 110 (series MS with VL) apparatus. The UV–vis and FL spectra were recorded as dilute solutions of the synthesized compounds in THF on Perkin Elmer Lambda 35 and Hitachi MPF-4 spectrophotometers accordingly. Microcells with an internal width of 1 and 10 mm were used, respectively. The DSC and TGA measurements were carried out on a Mettler DSC 30 calorimeter at a scan rate of 10 K/min. CV measurements were carried out by a three-electrode assembly cell from Bio-Logic SAS and a micro-AUTOLAB Type III potentiostat–galvanostat. The measurements were carried out with a glassy carbon electrode in dichloromethane solutions containing 0.1 M tetrabutylammonium perchlorate as electrolyte, $Ag/AgNO_3$ as the reference electrode and a Pt wire counter electrode.

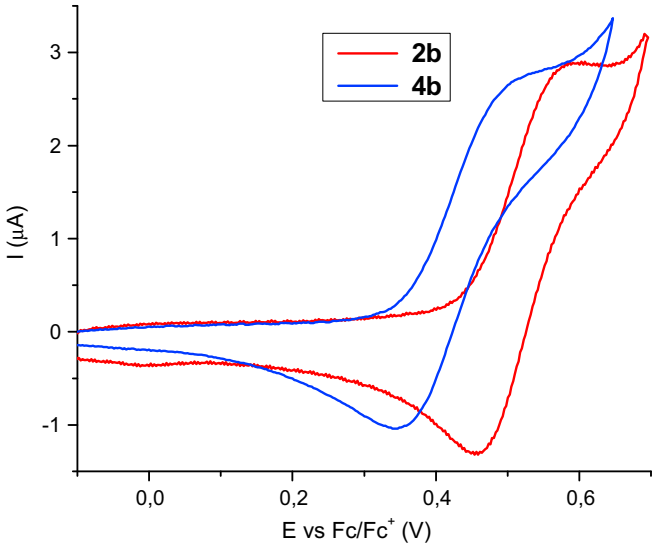

Figure 3. Cyclic voltammograms of **2b** (scan rate=50 mV s^{-1}) and **4b** (scan rate=20 mV s^{-1}) in argon-purged dichloromethane solutions.

Table 3
Hole mobility data for mixtures of **2a**,**b** and **4a**,**b** with PC-Z

Transport material, host polymer	d/μm	μ_0/cm^2 V^{-1} s^{-1}[a]	μ/cm^2 V^{-1} s^{-1}[b]	α/cm$^{1/2}$ V$^{-1/2}$
2a+PC-Z, 1:1	7	2×10^{-8}	1.1×10^{-5}	0.006
2b+PC-Z, 1:1	12	3×10^{-6}	6.9×10^{-5}	0.0031
4a+PC-Z, 1:2	12	3×10^{-8}	2.5×10^{-6}	0.0044
4b+PC-Z, 1:1	7.5	1×10^{-6}	8.1×10^{-5}	0.0044

[a] Mobility value at zero field strength.
[b] Mobility value at 10^6 V cm^{-1} field strength.

4.1.1. Ionization energy measurements. The ionization energy E_I of the layers of the synthesized compounds was measured by the electron photoemission in air method. The samples for the ionization energy measurement were prepared by dissolving materials in THF and were coated on Al plates pre-coated with ~0.5 μm thick methylmethacrylate and methacrylic acid copolymer adhesive layer. The thickness of the transporting material layer was 0.5–1 μm.

The samples were illuminated with monochromatic light from the quartz monochromator with a deuterium lamp. The power of the incident light beam was $(2–5)\times10^{-8}$ W. The negative voltage of

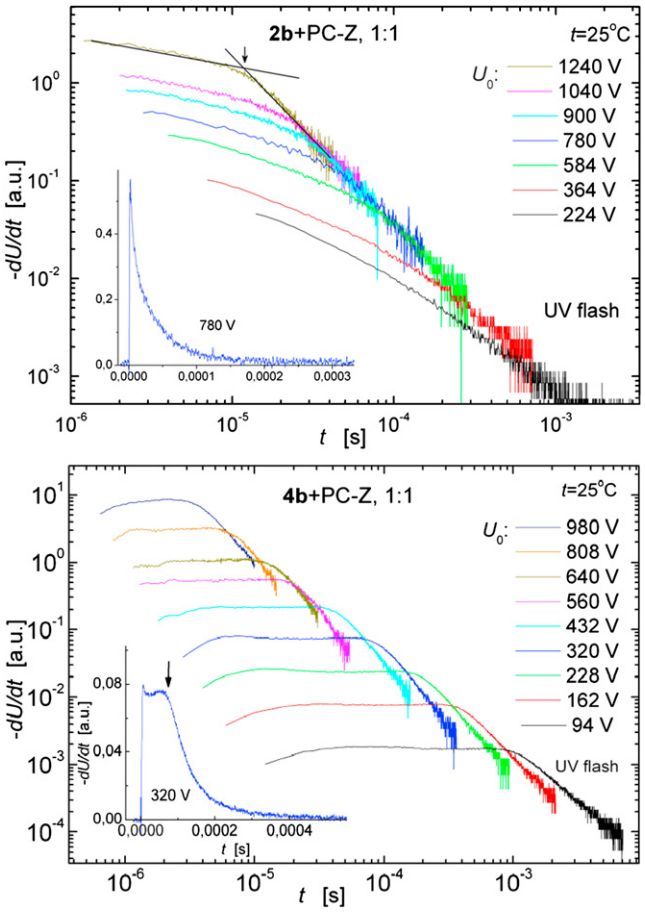

Figure 4. XTOF transients for the **2b** and **4b**. Insets show one transient curve in linear plot.

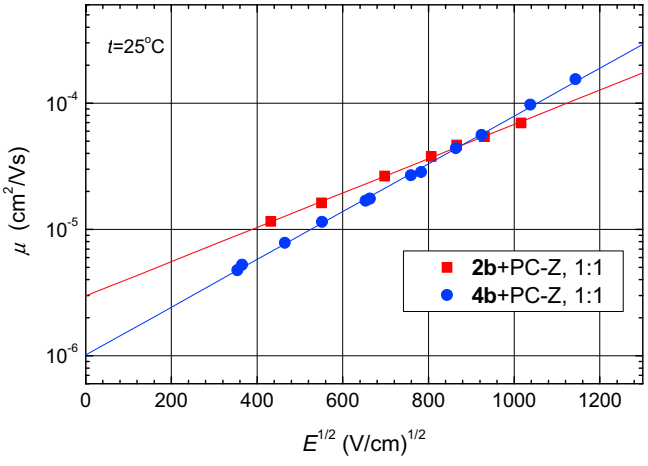

Figure 5. Electric field dependencies of the hole-drift mobilities (μ) in charge transport layers of compounds **2b** and **4b** doped in PC-Z (mass proportion 1:1).

–300 V was supplied to the sample substrate. The counter-electrode with the 4.5×15 mm^2 slit for illumination was placed at an 8 mm distance from the sample surface. The counter-electrode was connected to the input of the BK2-16 type electrometer, working in the open input regime, for the photocurrent measurement. The 10^{-15}—10^{-12} A strong photocurrent was flowing in the circuit under illumination. The photocurrent I is strongly dependent on the incident light photon energy $h\nu$. The $I^{0.5}=f(h\nu)$ dependence was plotted. Usually the dependence of the photocurrent on incident light quanta energy is well described by the linear relationship between $I^{0.5}$ and $h\nu$ near the threshold. The linear part of this dependence was extrapolated to the $h\nu$ axis and the E_I value was determined as the photon energy at the interception point.

4.1.2. Hole mobility measurements. The samples for mobility measurements were prepared from 1:1 mass proportion composition of the investigated compound with polycarbonate-Z (Iupilon Z-200 from Mitsubishi Gas Chemical Co.). The sample substrate was polyester film with conductive Al layer. The layer thickness was in the range 5–10 μm.

The hole-drift mobility was measured by the xerographic time-of-flight technique. Electric field was created by positive corona charging. The charge carriers were generated at the layer surface by illumination with pulses of nitrogen laser (pulse duration was 2 *ns*, wavelength 337 nm). The layer surface potential decrease as a result of pulse illumination was up to 1–5% of initial potential before illumination. The capacitance probe that was connected to the wide frequency band electrometer measured the speed of the surface potential decrease dU/dt. The transit time t_t was determined by the kink on the curve of the dU/dt transient in double logarithmic scale. The drift mobility was calculated by the formula $\mu=d^2/U_0t_t$, where d is the layer thickness, U_0—the surface potential at the moment of illumination.

4.2. Synthesis

*4.2.1. 1,3-Bis(2,2-diphenylethenyl)-9H-carbazol-2-ol (**1**).* 9*H*-Carbazol-2-ol (15 g, 0.082 mol) was dissolved in 1,4-dioxane (110 mL), (+/−)-camphor-10-sulfonic acid (19.04 g, 0.082 mol) was added and the mixture was heated at reflux for 20 min. Diphenylacetaldehyde (40.17 g, 0.205 mol) was next added and reflux continued (3 h). Water generated during the course of the reaction was removed with 4 Å molecular sieves. After termination of the reaction (TLC control, acetone/*n*-hexane, 7:18), the mixture was treated with ethyl acetate and washed with distilled water. The organic layer was dried over anhydrous $MgSO_4$, filtered and solvents were removed. The residue was purified by column chromatography using acetone/*n*-hexane (1:24 and 1:4 v/v) as eluent. Recrystallization of the residue from toluene yielded **1** (26.51 g, 60%) as a pale yellow powder, mp: 194–195 °C (recrystallized from toluene); [Found: C, 89.16; H, 5.50; N, 2.51. $C_{40}H_{29}NO$ requires C, 89.02; H, 5.42; N, 2.60%]; R_f (acetone/*n*-hexane, 7:18, v/v) 0.49; ν_{max}(KBr) 3537, 3440, 3077, 3056, 3028, 1625, 1611, 1594, 1490, 1444, 1183, 806, 779, 769, 760, 736, 701, 654 cm^{-1}; δ_H (300 MHz, $CDCl_3$) 7.57–7.50 (m, 1H), 7.47–7.09 (m, 25H), 7.08–6.97 (m, 2H), 5.31 (s, 1H); δ_C (75 MHz, $CDCl_3$) 150.5, 145.7, 143.5, 143.1, 142.9, 140.4, 139.68, 139.62, 137.4, 130.7, 129.8, 128.96, 128.74, 128.66, 128.49, 128.37, 128.09, 127.65, 126.18, 124.6, 123.8, 121.6, 120.5, 119.57, 119.36, 117.9, 116.7, 110.3, 107.4; MS(APCI$^+$, 20 V), *m*/*z*: 540 ($[M+H]^+$).

*4.2.2. 1,3-Bis(2,2-diphenylethenyl)-9-methyl-2-methoxycarbazol (**2a**).* Compound **1** (1.98 g, 0.004 mol) was dissolved in iodomethane (11.5 mL, 0.183 mol), 85% powdered KOH (1.45 g, 0.022 mol) and anhydrous Na_2SO_4 (0.78 g, 0.006 mol) were added and the reaction mixture was heated at reflux for 3 h. After termination of the reaction (TLC control, acetone/*n*-hexane, 1:4), the mixture was treated with ethyl acetate and washed with distilled water. The organic layer was dried over anhydrous $MgSO_4$, filtered, solvents were removed. Recrystallization of the residue from ethyl acetate yielded **2a** (1.29 g, 62%) as a pale yellow powder, mp: 210–212 °C (recrystallized from ethyl acetate); [Found: C, 88.76; H, 5.93; N, 2.51. $C_{42}H_{33}NO$ requires C, 88.86; H, 5.86; N, 2.47%]; R_f (acetone/*n*-hexane, 1:4, v/v) 0.49; ν_{max}(KBr) 3054, 3028, 2997, 2927, 1621, 1589, 1485, 1464, 1443, 1238, 1217, 1052, 1031, 774, 764, 753, 742, 725, 698 cm^{-1}; δ_H (300 MHz, $CDCl_3$) 7.49–7.19 (m, 21H), 7.16–7.04 (m, 6H), 3.90 (s, 3H), 3.79 (s, 3H); δ_C (75 MHz, $CDCl_3$) 156.2, 146.1,

143.88, 143.46, 142.5, 141.24, 141.06, 139.86, 139.19, 130.9, 129.9, 128.71, 128.62, 128.57, 128.30, 127.94, 127.81, 127.45, 127.31, 127.27, 125.1, 124.2, 123.1, 122.9, 121.54, 121.16, 119.53, 119.42, 119.22, 115.1, 108.7, 61.6, 32.1; MS(APCI$^+$, 20 V), m/z: 568 ([M+H]$^+$).

*4.2.3. 1,3-Bis(2,2-diphenylethenyl)-9-propyl-2-propoxycarbazol (**2b**).* Compound **2b** was prepared and isolated according to the same procedure as **2a**, except that **1** (12 g, 0.022 mol), 1-brompropane (100 mL, 1.1 mol), 85% powdered KOH (8.81 g, 0.133 mol) and anhydrous Na_2SO_4 (4.74 g, 0.033 mol) of were used. Recrystallization of the residue from ethyl acetate yielded **2b** (10.82 g, 78%) as a pale yellow powder, mp: 140–141 °C (recrystallized from ethyl acetate); [Found: C, 88.50; H, 6.54; N, 2.20. $C_{46}H_{41}NO$ requires C, 88.57; H, 6.62; N, 2.25%]; R_f (acetone/*n*-hexane, 1:4, v/v) 0.74; ν_{max}(KBr) 3077, 3055, 3020, 2990, 2958, 2948, 2877, 2866, 1621, 1595, 1579, 1494, 1479, 1467, 1457, 1056, 1005, 893, 774, 767, 749, 726, 715, 696 cm^{-1}; δ_H (300 MHz, $CDCl_3$) 7.49–7.15 (m, 21H), 7.12–7.00 (m, 6H), 4.65–4.46 (m, 1H), 4.28–4.09 (m, 1H), 4.00–3.67 (m, 2H), 1.85–1.63 (m, 4H), 0.91 (t, J=7.4 Hz, 3H), 0.78 (t, J=7.4 Hz, 3H); δ_C (75 MHz, $CDCl_3$) 155.2, 146.2, 143.85, 143.61, 141.73, 141.16, 140.5, 139.8, 138.6, 130.9, 129.9, 128.76, 128.52, 128.37, 128.28, 127.82, 127.73, 127.37, 127.23, 127.15, 124.96, 124.35, 123.31, 123.13, 121.5, 120.9, 119.57, 119.24, 119.11, 114.8, 108.9, 75.9, 46.1, 23.86, 23.81, 11.5, 10.9; MS(APCI$^+$, 20 V), m/z: 624 ([M+H]$^+$).

*4.2.4. 9-Methyl-2-methoxycarbazol (**3a**).* 9*H*-Carbazol-2-ol (8 g, 0.044 mol) was dissolved in DMF (30 mL), iodomethane (16.3 mL, 0.262 mol), 85% powdered KOH (11.62 g, 0.176 mol) and anhydrous Na_2SO_4 (6.25 g, 0.044 mol) were added and reaction mixture stirred at room temperature (10 min). After termination of the reaction (TLC control, acetone/*n*-hexane, 1:4), water was added and the precipitate was filtered off, washed with water and ethanol. Recrystallization of the residue from acetone yielded **3a** (8.05 g, 87%) as a pale brown powder, mp: 98–99 °C (recrystallized from acetone); [Found: C, 79.66; H, 6.14; N, 6.55. $C_{14}H_{13}NO$ requires C, 79.59; H, 6.20; N, 6.63%]; R_f (acetone/*n*-hexane, 1:4, v/v) 0.44; ν_{max}(KBr) 3010, 2965, 2944, 2909, 2836, 1628, 1608, 1569, 1503, 1462, 1443, 1306, 1163, 764, 746, 727 cm^{-1}; δ_H (300 MHz, $CDCl_3$) 8.03–7.91 (m, 2H), 7.44–7.29 (m, 2H), 7.26–7.15 (m, 1H), 6.88–6.81 (m, 2H), 3.93 (s, 3H), 3.78 (s, 3H); δ_C (75 MHz, $CDCl_3$) 159.3, 142.5, 141.2, 124.5, 123.1, 121.2, 119.57, 119.11, 116.8, 108.3, 107.4, 92.9, 55.8, 29.2; MS(APCI$^+$, 20 V), m/z: 212 ([M+H]$^+$).

*4.2.5. 9-Propyl-2-propoxycarbazol (**3b**).* Compound **3b** was prepared and isolated according to the same procedure as **3a**, except that 9*H*-carbazol-2-ol (25 g, 0.137 mol), 1-brompropane (74.4 mL, 0.819 mol), 85% powdered KOH (54.04 g, 0.819 mol) and of anhydrous Na_2SO_4 (29.09 g, 0.205 mol) were used. Recrystallization of the residue from methanol yielded **3b** (35.31 g, 97%) as a pale brown powder, mp: 38–39 °C (recrystallized from methanol); [Found: C, 80.78; H, 7.84; N, 5.30. $C_{18}H_{21}NO$ requires C, 80.86; H, 7.92; N, 5.24%]; R_f (acetone/*n*-hexane, 1:4, v/v) 0.85; ν_{max}(KBr) 3043, 3024, 2965, 2935, 2875, 1628, 1600, 1573, 1498, 1467, 1459, 1194, 1117, 768, 760, 746 cm^{-1}; δ_H (300 MHz, $CDCl_3$) 7.97 (d, J=7.6 Hz, 1H), 7.92 (d, J=8.3 Hz, 1H), 7.41–7.29 (m, 2H), 7.23–7.12 (m, 1H), 6,87–6,79 (m, 2H), 4.17 (t, J=7.2 Hz, 2H), 4.03 (t, J=6.6 Hz, 2H), 1.95–1.79 (m, 4H), 1.08 (t, J=7.4 Hz, 3H), 0.96 (t, J=7.4 Hz, 3H); δ_C (75 MHz, $CDCl_3$) 158.7, 142.1, 140.8, 124.4, 123.2, 121.1, 119.6, 118.9, 116.8, 108.6, 107.6, 94.2, 70.2, 44.7, 22.97, 22.35, 12.0, 10.8; MS(APCI$^+$, 20 V), m/z: 268 ([M+H]$^+$).

*4.2.6. 3,6-Bis(2,2-diphenylethenyl)-9-methyl-2-methoxycarbazol (**4a**).* Compound **3a** (6 g, 0.028 mol) was dissolved in toluene (30 mL), (+/−)-camphor-10-sulfonic acid (6.5 g, 0.028 mol) was added and the mixture was heated at reflux for 20 min. Afterwards diphenylacetaldehyde (13.93 g, 0.071 mol) was added and reflux continued (3 h) using a Dean–Stark trap. After termination of the reaction (TLC control, acetone/*n*-hexane, 1:4), the mixture was treated with ethyl acetate and washed with distilled water. The organic layer was dried over anhydrous $MgSO_4$, filtered and solvents were removed. The residue was purified by column chromatography using acetone/dichloromethane/*n*-hexane (0.5:0.5:4 v/v/v) as eluent. Recrystallization of the residue from ethyl acetate yielded **4a** (10.96 g, 68%) as a pale yellow powder, mp: 228–230 °C (recrystallized from ethyl acetate); [Found: C, 88.80; H, 5.78; N, 2.54. $C_{42}H_{33}NO$ requires C, 88.86; H, 5.86; N, 2.47%]; R_f (acetone/*n*-hexane, 1:4, v/v) 0.30; ν_{max}(KBr) 3076, 3055, 3020, 2933, 2832, 1632, 1600, 1591, 1492, 1473, 1443, 1253, 1212, 1208, 1121, 1059, 893, 803, 778, 761, 741, 731, 697 cm^{-1}; δ_H (300 MHz, $CDCl_3$) 7.45–7.17 (m, 23H), 7.07 (s, 1H), 7,02–6,92 (m, 2H), 6,70 (s, 1H), 3,92 (s, 3H), 3,68 (s, 3H); δ_C (75 MHz, $CDCl_3$) 157.9, 144.22, 144.05, 141.70, 141.22, 141.12, 140.84, 140.02, 130.75, 130.72, 129.38, 128.88, 128.78, 128.67, 128.36, 128.26, 127.98, 127.60, 127.33, 127.25, 127.20, 126.25, 124.1, 123.0, 121.95, 121.01, 119.5, 115.7, 107.7, 90.6, 55.9, 29.2; MS(APCI$^+$, 20 V), m/z: 568 ([M+H]$^+$).

*4.2.7. 3,6-Bis(2,2-diphenylethenyl)-9-propyl-2-propoxycarbazol (**4b**).* Compound **4b** was prepared according to the same procedure as **4a** except that **3b** (5 g, 0.019 mol), (+/−)-camphor-10-sulfonic acid (4.41 g, 0.019 mol) and diphenylacetaldehyde (9.17 g, 0.047 mol) were used. After termination of the reaction (TLC control, acetone/*n*-hexane, 1:4), the mixture was treated with ethyl acetate and washed with distilled water. The organic layer was dried over anhydrous $MgSO_4$, filtered and solvents were removed. Recrystallization of the residue from ethylmethylketone yielded **4b** (8.98 g, 77%) as a pale yellow powder, mp: 193–194 °C (recrystallized from ethylmethylketone); [Found: C, 88.65; H, 6.57; N, 2.32. $C_{46}H_{41}NO$ requires C, 88.57; H, 6.62; N, 2.25%]; R_f (acetone/*n*-hexane, 1:4, v/v) 0.58; ν_{max}(KBr) 3077, 3055, 3020, 2964, 2873, 1630, 1592, 1491, 1485, 1472, 1442, 1260, 1199, 1125, 1069, 798, 776, 758, 737, 724, 702, 694 cm^{-1}; δ_H (300 MHz, $CDCl_3$) 7.44–7.17, (m, 23H), 7.05 (s, 1H), 6.99–6.88 (m, 2H), 6.69 (s, 1H), 4.14–3.97 (m, 4H), 1.91–1.71 (m, 4H), 1.08 (t, J=7.4 Hz, 3H), 0.92 (t, J=7.4 Hz, 3H); δ_C (75 MHz, $CDCl_3$) 157.4, 144.38, 144.14, 141.35, 141.24, 141.16, 140.24, 139.88, 139.67, 130.79, 130.73, 129.44, 128.89, 128.78, 128.64, 128.36, 128.29, 127.89, 127.62, 127.31, 127.21, 127.05, 126.0, 124.0, 123.2, 121.89, 121.15, 119.7, 115.8, 107.9, 92.0, 70.6, 44.8, 22.90, 22.42, 12.0, 11.0; MS(APCI$^+$, 20 V), m/z: 624 ([M+H]$^+$).

*4.2.8. 1,3-Bis(2,2-diphenylethenyl)-6-methanoyl-9-propyl-2-propoxycarbazol (**5**).* DMF (2.49 mL, 0.032 mol) was cooled in a ice/salt bath to 0 °C and $POCl_3$ (3 mL, 0.032 mol) was slowly added. During the addition of $POCl_3$ temperature of mixture was not allowed to rise above 5 °C. After addition of $POCl_3$ the reaction mixture was allowed to warm to room temperature and **2b** (3.35 g, 0.005 mol), dissolved in DMF (20 mL), was added. The mixture was heated for 3 h at 90 °C. After termination of the reaction (TLC control, acetone/*n*-hexane, 7:18), hot reaction mixture was poured into a beaker with ice, neutralized by adding sodium acetate (9.58 g; 0.12 mol) solution in water and allowed to stand at 5 °C for 24 h. Recrystallization of the residue from ethanol/ethyl acetate, 1:3 yielded **5** (3.42 g, 98%) as pale yellow powder, mp: 194–195 °C (recrystallized from ethanol/ethyl acetate, 1:3); [Found: C, 86.45; H, 6.42; N, 2.24. $C_{47}H_{41}NO_2$ requires C, 86.60; H, 6.34; N, 2.15%]; R_f (acetone/*n*-hexane, 7:18, v/v) 0.59; ν_{max}(KBr) 3054, 3024, 2961, 2934, 2874, 2820, 1686, 1621, 1590, 1572, 1489, 1468, 1442, 1340, 1199, 1133, 1061, 1032, 807, 799, 772, 763, 737, 727, 698 cm^{-1}; δ_H (300 MHz, $CDCl_3$) 9.95 (s, 1H), 7.95 (d, J=1.5 Hz, 1H), 7.86 (dd, J_1=8.6 Hz, J_2=1.5 Hz, 1H), 7.50–6.98 (m, 24H), 4.70–4.50 (m, 1H), 4.31–4.09 (m, 1H), 4.04–3.72 (m, 2H), 1.92–1.56 (m, 4H), 0.92 (t, J=7.4 Hz, 3H), 0.81 (t, J=7.4 Hz, 3H); δ_C (75 MHz, $CDCl_3$) 191.8, 156.0, 146.8, 145.4, 143.58, 143.26, 141.7, 140.8, 139.88, 139.55, 139.10, 130.85, 129.81,

128.83, 128.60, 128.34, 128.32, 128.04, 127.81, 127.70, 127.45, 127.42, 126.50, 124.9, 123.95, 123.48, 123.09, 121.3, 120.6, 119.3, 115.8, 109.2, 75.9, 46.3, 23.81, 23.79, 11.5, 10.9; MS(APCI$^+$, 20 V), *m*/*z*: 652 ([M+H]$^+$).

Crystallographic data (excluding structure factors) for the structures in this paper have been deposited with the Cambridge Crystallographic Data Centre as supplementary publication numbers CCDC 741268 and 741269. These data can be obtained free of charge via www.ccdc.cam.ac.uk/data_request/cif, or by emailing data_request@ccdc.cam.ac.uk, or by contacting The Cambridge Crystallographic Data Centre, 12, Union Road, Cambridge CB2 1EZ, UK; fax: +44 1223 336033.

Acknowledgements

Financial support by the Lithuanian Science and Studies Foundation is gratefully acknowledged. Habil. Dr. V. Gaidelis from the Department of Solid State electronics, Vilnius University is thanked for the ionization energy measurements.

Supplementary data

Supplementary data associated with this article can be found in the online version at doi:10.1016/j.tet.2010.02.086.

References and notes

1. (a) Forrest, S. R. *Nature* **2004**, *428*, 911; (b) Shirota, Y. *J. Mater. Chem.* **2005**, *15*, 75; (c) *Organic Light-Emitting Devices, Synthesis, Properties, and Applications*; Müllen, K., Scherf, U., Eds.; Wiley-VCH: Weinheim, 2006; (d) *Organic Photovoltaics, Mechanisms, Materials and Devices*; Sun, S. S., Sariciftci, N. S., Eds.; CRC: New York, NY, 2005; (e) Mas-Torrent, M.; Rovira, C. *J. Mater. Chem.* **2006**, *16*, 433.
2. (a) Shirota, Y.; Kageyama, H. *Chem. Rev.* **2007**, *107*, 953; (b) Grazulevicius, J. V.; Strohriegl, P. *Adv. Mater.* **2002**, *14*, 1439; (c) Sonntag, M.; Kreger, K.; Hanft, D.; Strohriegl, P. *Chem. Mater.* **2005**, *17*, 3031.
3. (a) Adhikari, R. M.; Mondal, R.; Shah, B. K.; Neckers, D. C. *J. Org. Chem.* **2007**, *72*, 4727; (b) Zhao, Z.; Zhang, P.; Wang, F.; Wang, Z.; Lu, P.; Tian, W. *Chem. Phys. Lett.* **2006**, *423*, 293; (c) Shen, J.-Y.; Yang, X.-L.; Huang, T.-H.; Lin, J. T.; Ke, T.-H.; Chen, L.-Y.; Wu, C.-C.; Yeh, M.-C. P. *Adv. Funct. Mater.* **2007**, *17*, 983.
4. (a) Liu, Y.; Nishiura, M.; Wang, Y.; Hou, Z. *J. Am. Chem. Soc.* **2006**, *128*, 5592; (b) Li, J. Y.; Liu, D.; Ma, C. W.; Lengyel, O.; Lee, C.-S.; Tung, C.-H.; Lee, S. T. *Adv. Mater.* **2004**, *16*, 1583; (c) Zhao, Z.; Zhao, Y.; Lu, P.; Tian, W. *J. Phys. Chem. C* **2007**, *111*, 6883.
5. (a) Liu, B.; Yu, W.; Lai, Y.; Huang, W. *Chem. Mater.* **2001**, *13*, 1984; (b) Xia, C.; Advincula, R. C. *Macromolecules* **2001**, *34*, 5854; (c) Stephan, O.; Vial, J.-C. *Synth. Met.* **1999**, *106*, 115; (d) Promarak, V.; Ichikawa, M.; Sudyoadsuk, T.; Saengsuwan, S.; Jungsuttiwong, S.; Keawin, T. *Synth. Met.* **2007**, *157*, 17; (e) Li, J.; Ma, C.; Tang, J.; Lee, C.-S.; Lee, S. T. *Chem. Mater.* **2005**, *17*, 615; (f) Qian Zhang, Q.; Chen, J.; Cheng, Y.; Wang, L.; Ma, D.; Jing, X.; Wang, F. *J. Mater. Chem.* **2004**, *14*, 895.
6. (a) Chen, Y.-C.; Huang, G.-S.; Hsiao, C.-C.; Chen, S.-A. *J. Am. Chem. Soc.* **2006**, *128*, 5592; (b) Tsai, M.-H.; Hong, Y.-H.; Chang, C.-H.; Su, H.-C.; Wu, C.-C.; Matoliukstyte, A.; Simokaitiene, J.; Grigalevicius, S.; Grazulevicius, J. V.; Hsu, C.-P. *Adv. Mater.* **2007**, *19*, 862; (c) Shih, P.-I.; Chiang, C.-L.; Dixit, A. K.; Chen, C.-K.; Yuan, M.-C.; Lee, R.-Y.; Chen, C.-T.; Diau, E. W.-G.; Shu, C.-F. *Org. Lett.* **2006**, *8*, 2799.
7. (a) Sonntag, M.; Strohriegl, P. *Chem. Mater.* **2004**, *16*, 4736; (b) Morin, J.-F.; Leclerc, M.; Adès, D.; Siove, A. *Macromol. Rapid Commun.* **2005**, *26*, 761; (c) Matoliukstyte, A.; Burbulis, E.; Grazulevicius, J. V.; Gaidelis, V.; Jankauskas, V. *Synth. Met.* **2008**, *158*, 462; (d) Lygaitis, R.; Getautis, V.; Grazulevicius, J. V. *Chem. Soc. Rev.* **2008**, *37*, 770; (e) Bubniene, G.; Malinauskas, T.; Stanisauskaite, A.; Jankauskas, V.; Getautis, V. *Synth. Met.* **2009**, *159*, 1695; (f) Getautis, V.; Daskeviciene, M.; Malinauskas, T.; Stanisauskaite, A.; Stumbraite, J. *Molecules* **2006**, *11*, 64.
8. Bubniene, G.; Stanisauskaite, A.; Getautis, V; Daskeviciene, M.; Jankauskas, V.; Sidaravicius; J. Abstract Book, International Conference on Organic Synthesis, Vilnius, Lithuania, June 29–July 2, 2008; Vilnius University: Vilnius, 2008; PO 19.
9. (a) Kirkus, M.; Tsai, M. H.; Grazulevicius, J. V.; Wu, C. C.; Chi, L. C.; Wong, K. T. *Synth. Met.* **2009**, *159*, 729; (b) Miyamoto, E.; Yamaguchi, Y.; Yokoyama, M. *Electrophotography* **1989**, *28*, 364; (c) Cordona, M.; Ley, L. *Top. Appl. Phys.* **1978**, *26*, 1.
10. (a) Vaezi-Nejad, S. M. *Int. J. Electron.* **1987**, *62*, 361; (b) Archie, Y.; Chan, C.; Juhasz, C. *Int. J. Electron.* **1987**, *62*, 625.